11-18-2016

Spin–Lattice Coupling in [Ni(HF2)(pyrazine)2]SbF6 Involving the HF2 − Superexchange Pathway

Kenneth Robert O'Neal
koneal5@vols.utk.edu

Brian S. Holinsworth
University of Tennessee, Knoxville

Z Chen
National High Magnetic Field Laboratory

P K. Peterson
Eastern Washington University

K E. Carreiro
Eastern Washington University

See next page for additional authors

Spin-lattice coupling in $[Ni(HF_2)(pyrazine)_2]SbF_6$ involving the HF_2^- superexchange pathway

Kenneth R. O'Neal,[†] Brian S. Holinsworth,[†] Zhiguo Chen,[‡] Peter K. Peterson,[¶] Kimberly E. Carreiro,[¶] Jamie L. Manson,[¶] Mike H. Whangbo,[§] Zhiqiang Li,[‡] Zhenxian Liu,[∥] and Janice L. Musfeldt*[,†]

†*Department of Chemistry, University of Tennessee, Knoxville, Tennessee 37996, USA*

‡*National High Magnetic Field Laboratory, Tallahassee, Florida 32310, USA*

¶*Department of Chemistry and Biochemistry, Eastern Washington University, Cheney, Washington 99004, United States*

§*Department of Chemistry, North Carolina State University, Raleigh, North Carolina 27695, USA*

∥*Geophysical Laboratory, Carnegie Institution of Washington, Washington D.C. 20015 USA*

⊥*Department of Physics, University of Tennessee, Knoxville, Tennessee 37996, USA*

E-mail: musfeldt@utk.edu

Abstract

Magnetoelastic coupling in the quantum magnet $[Ni(HF_2)(pyrazine)_2]SbF_6$ is investigated via vibrational spectroscopy using temperature, magnetic field, and pressure as tuning parameters. While pyrazine is known to be a malleable magnetic superexchange ligand, we find that HF_2^- is surprisingly sensitive to external stimuli and actively involved in the magnetic quantum phase transition and a series of pressure-induced

structural distortions. The amplified spin-lattice interactions involving the bifluoride ligand are discussed in terms of the intra- and inter-planar magnetic energy scales.

KEYWORDS: magnetoelastic coupling, metal halide coordination polymer, hydrogen bonding, quantum magnet, external stimuli

Introduction

Metal-halide coordination polymers provide a superb platform for testing the capability of various ligands to manipulate and control properties such as dimensionality, electronic structure, and magnetism. Within this broad class of materials, heterocyclic ligands (such as pyrazine) often connect transition metal centers into extended arrays[1,2] and can support magnetic superexchange, leading to a soft lattice and overall low energy scales. Recently, ligands such as HF_2^- and $H_2F_3^-$ have drawn attention[2] because strong hydrogen bonding can also support magnetic interactions.[3] However, in most mixed ligand systems, the role of hydrogen bonded moieties is typically eclipsed by stronger superexchange mediated through the organic ligands.[1] Table 1 illustrates the intra- and interplane exchange interactions (J's) for a few representative systems.[4] Most materials of this type sport $|J_{inter}/J_{intra}|$ ratios that are less than or close to one, leading to dominant intraplane interactions especially in the Cu(II) systems. $[Ni(HF_2)(pyz)_2]SbF_6$ (pyz = pyrazine) is different. Here, the inter- and intraplane superexchange strengths are reversed, with the Ni-FHF-Ni interaction being substantially stronger,[3] making it an ideal platform with which to explore the effects of external stimuli on the HF_2^- ligand which consists of the strongest known hydrogen bonds.

Table 1: Summary of superexchange strengths in representative coordination polymers highlighting the strong interplane coupling and unique $|J_{inter}/J_{intra}|$ ratio in $[Ni(HF_2)(pyz)_2]SbF_6$.

Material	$\lvert J_{intra}\rvert$ (K)	$\lvert J_{inter}\rvert$ (K)	$\lvert J_{inter}/J_{intra}\rvert$	Reference
$[Ni(HF_2)(pyz)_2]SbF_6$	1	11.3	11	5
$[Cu(HF_2)(pyz)_2]SbF_6$	13.3	0.1	9×10^{-3}	6
$[Co(HF_2)(pyz)_2]SbF_6$	7	7	1	6
$NiCl_2(pyz)_2$	0.49	<0.05	<0.1	7
$NiI_2(pyz)_2$	<1.19	>1.19	>1	7
$CuF_2(H_2O)_2(pyz)$	5.8	2×10^{-3}	4×10^{-4}	8

$[Ni(HF_2)(pyz)_2]SbF_6$ combines pyrazine and HF_2^- ligands in a robust three-dimensional tetragonal ($P4/nmm$) framework.[3] Nickel(II) centers are connected by pyrazine rings within the ab-plane whereas HF_2^- form bridges between the planes along the c-direction. Hexafluoroantimonate counterions (SbF_6^-) reside in the interior sites to further stabilize the structure

(Fig. 1). These HF_2^- linkages facilitate magnetic exchange, and in $[Ni(HF_2)(pyz)_2]SbF_6$ they result in quasi-one-dimensional (Q1D) antiferromagnetic chains that ultimately undergo long-range order below $T_N = 12.2$ K due to an additional, albeit weaker magnetic exchange through the pyz bridges.[3] This T_N is among the highest magnetic ordering temperatures for any metal-pyrazine coordination polymer,[1] allowing the system to be unambiguously studied in the fully ordered state. Moreover, a Q1D magnet embedded within a rigid three-dimensional crystal structure illustrates, yet again, that superexchange patterns and lattice dimensionality do not always go hand-in-hand.[9] A relatively unexplored magnetic field-driven quantum phase transition also takes place at 37.4 T, above which the magnetization saturates.[3] The dual structural and magnetic role of HF_2^- in this particular quantum magnet presents an ideal opportunity to reveal energy transfer mechanisms in a system with strong inter-layer interactions mediated by hydrogen bonds.

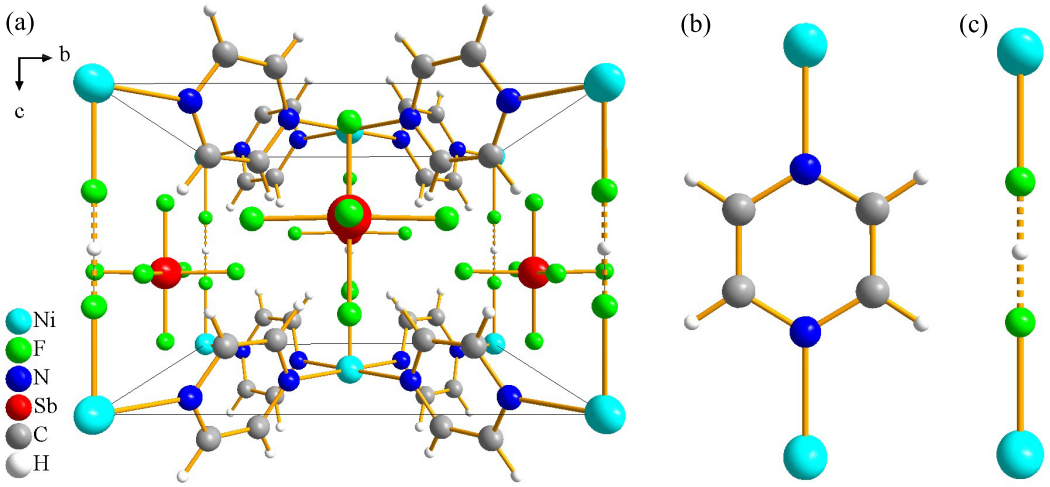

Figure 1: (a) View of the tetragonal crystal structure (*P4/nmm*) of $[Ni(HF_2)(pyz)_2]SbF_6$ at 300 K along the *a*-axis. (b) Close-up view of pyrazine rings that link Ni(II) centers within the *ab*-plane. (c) HF_2^- inter-plane bridging ligands along the *c*-axis are held together by notably strong hydrogen bonding. These linkages result in a three-dimensional structure (Ni-pyrazine planes) with quasi-one-dimensional magnetism (through the HF_2^-).[3]

In the present work, we measured the vibrational response of $[Ni(HF_2)(pyz)_2]SbF_6$ as a function of temperature, magnetic field, and pressure in order to explore spin-lattice coupling mediated by the unique hydrogen bonded HF_2^- ligand as well as the pyrazine rings.

Like the copper halides,[10–12] applied field distorts the pyrazine rings which reduces antiferromagnetic interactions and stabilizes the fully polarized state. Strikingly, the HF_2^- ligand also displays field-induced absorption changes on the order of 7%, indicating that distortions of this superexchange pathway are also required to achieve the fully polarized state. At the same time, pressure drives a structural phase transition at 3 GPa as well as more local distortions at 1 and 6 GPa that involve both pyrazine and HF_2^- ligands. We argue that the 3 GPa transition is most likely to modify the long range ordered state. What distinguishes this work from prior efforts[10,11,13] is the rare combination of physical tuning techniques brought together to explore the rich temperature-field-pressure phase space in $[Ni(HF_2)(pyz)_2]SbF_6$.[12] What emerges from this unique approach to exploring spin-lattice coupling processes is the finding that that while pyrazine is known to be a flexible superexchange ligand,[10–12] HF_2^- is surprisingly sensitive to external stimuli when inter-layer energy scales are important ($|J_{inter}/J_{intra}| > 1$).

Materials and methods

$[Ni(HF_2)(pyz)_2]SbF_6$ was synthesized by self-assembly in an aqueous solution as described previously.[3] Polycrystalline sample was mixed with a matrix as appropriate for infrared transmittance measurements (15-5000 cm^{-1}; 1 cm^{-1} resolution; 4.2-300 K). Absorption was calculated as $\alpha(\omega) = \frac{-1}{hd}\ln(T(\omega))$, where $T(\omega)$ is the measured transmittance, h is the sample loading, and d is thickness. High field infrared measurements were performed in a resistive magnet at 4.2 K and magnetic fields up to 35 T at the National High Magnetic Field Laboratory. Absorption differences, $\Delta\alpha = \alpha(\omega,\ B) - \alpha(\omega,\ B = 0\ \mathrm{T})$, are used to present the data in order to eliminate spectral commonalities. High pressure spectroscopies were carried out at the National Synchrotron Light Source at Brookhaven National Laboratory in order to take advantage of the high brightness infrared light.[14] Ruby fluorescence was used to measure pressure inside the diamond anvil cell.[15] Pressure-induced distortions are reversible

upon release of the pressure. Standard peak fitting procedures were employed as appropriate. Calculations of mode frequencies, symmetries, and displacements patterns were carried out using density functional theory as implemented in Spartan. Spin density distributions for the antiferromagnetic and ferromagnetic states were calculated using density functional theory and the Vienna *ab initio* simulation package.[16–20]

Results and discussion

Magnetoelastic coupling across the field-driven quantum phase transition

Like many transition metal halide framework materials, the infrared spectrum of $[Ni(HF_2)(pyz)_2]SbF_6$ displays a large number of vibrational modes.[3,21] In order to simplify our discussion, we focus on features that are sensitive to external stimuli, namely the out-of-plane pyrazine deformations centered at 490 and 820 cm^{-1} [Fig. 2 (a)] and the HF_2^- bending and asymmetric stretch(es) between 1200 and 1600 cm^{-1} [Fig. 2 (b)]. The variable temperature spectra show a gradual hardening of most modes down to 4.2 K, in line with the lack of structural transitions down to 17 K reported from x-ray studies.[3] Other classes of materials, such as oxides and chalcogenides, often require lattice distortions to establish long-range magnetic ordering,[22–26] but no local lattice distortions appear through the 12.2 K ordering temperature.

Magnetic field drives a quantum phase transition in $[Ni(HF_2)(pyz)_2]SbF_6$ at 37.4 T.[3] The pyrazine out-of-plane bending modes are quite sensitive to the changing microscopic spin pattern - an indication of spin-lattice coupling. The overall softening of these features is easily seen in the field-induced absorption difference, $\Delta\alpha$, [Fig. 2 (c)] where even at 5 T, there is a clear deviation from the baseline. The field-induced absorption difference continues to grow in magnitude with increasing field. Unfortunately, the quantum critical transition is just beyond the range of powered resistive magnets so the absorption difference does not

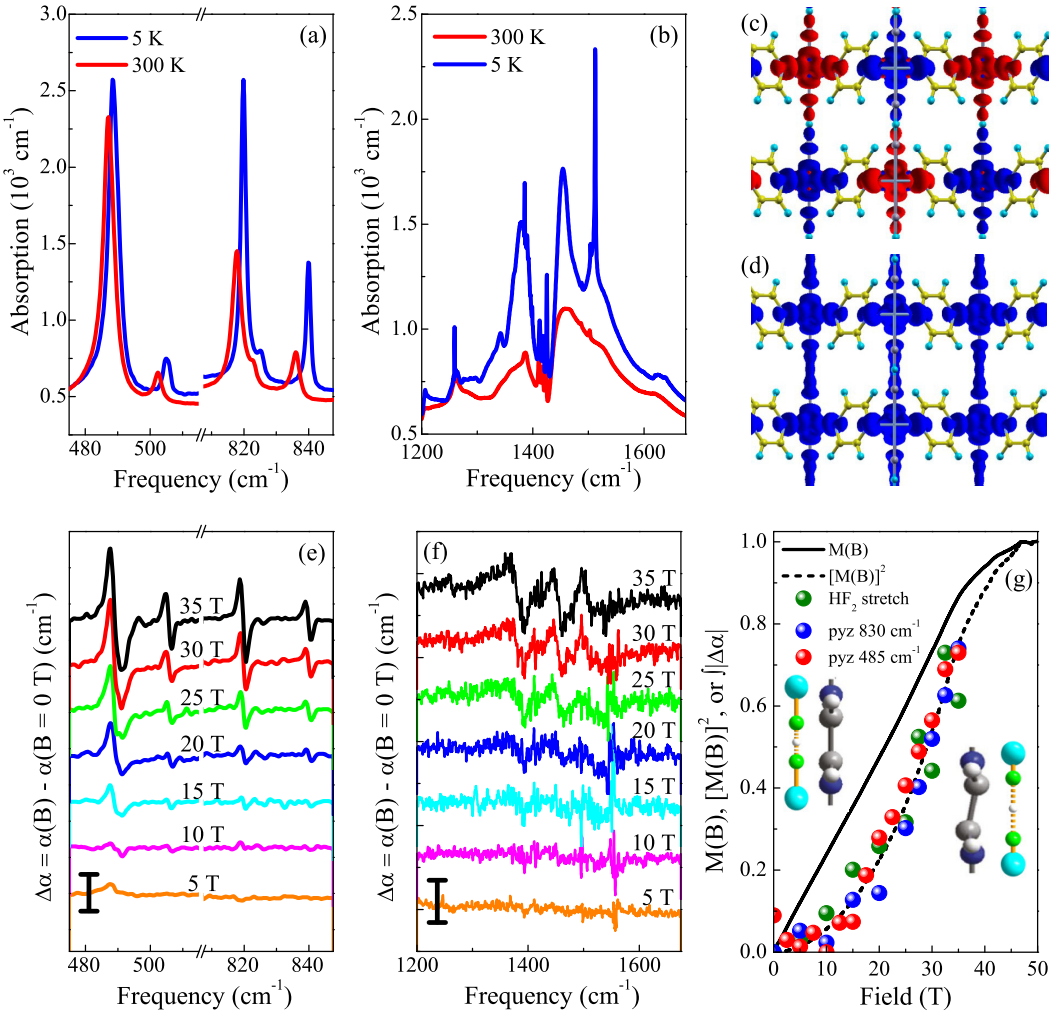

Figure 2: Close-up views of the infrared absorption spectrum of $[Ni(HF_2)(pyz)_2]SbF_6$ at 300 and 5 K for the (a) pyrazine out-of-plane and (b) HF_2^- modes. Calculated spin-densities of the (c) antiferromagnetic and (d) ferromagnetic states. Magnetic field-induced absorption differences for the (e) pyrazine and (f) HF_2^- features. Scale bars represent 500 and 100 cm^{-1}, respectively. (g) Comparison of integrated absorption difference to magnetization[3] and magnetization squared. These quantities are normalized in order to draw comparisons. Insets are the HF_2^- and pyrazine ring in the (left) low field and (right) distorted high field states to emphasize the field-induced changes.

saturate by 35 T. Nevertheless, the overall trend is quite clear. Prior estimates in chemically similar $Cu(pyz)_2HF_2BF_4$ indicate that a 1° out-of-plane bend of the pyrazine ring can be accommodated in resistive magnet at full field; such a hypothetical distortion changes J by approximately 3%.[10]

Magnetic field-induced changes in the higher frequency HF_2^- bending and asymmetric

stretching modes are shown in Fig. 2 (f). The derivative-like absorption difference features are not clearly seen above the background noise level until 15 T, although above this field the derivative-like lineshape reveals that these modes soften in response to the collective transition. The absence of new spectral features related to the development of an asymmetric HF_2^- linkage (for instance, movement of the central H)[27] indicates that the ligand remains symmetric across the magnetic quantum phase transition. With symmetry breaking ruled out, hydrogen bonding or bond length modifications must account for the observed mode softening in applied field. Stronger hydrogen bonding typically reduces mode frequencies.[28?,29] Bond length modifications can, however, also lower vibrational frequencies. In this scenario, mode softening is expected to relax the HF_2^- ligand, thereby reducing the antiferromagnetic exchange interactions in the inter-plane direction.[2,10] Since $|J_{inter}/J_{intra}| = 11$,[30] this is the dominant antiferromagnetic superexchange path that must be diminished in order to saturate the magnetization. We therefore assign the field-induced absorption differences of the HF_2^--related modes to the development of longer bifluoride ligands under high field. This is shown schematically in Fig. 2 (g). Based on a field-induced frequency shift on the order of 2 cm^{-1}, we estimate that the H···F bond lengthens from 1.150 to approximately 1.152 Å at 35 T.[30]

In order to quantify spin-lattice effects in $[Ni(HF_2)(pyz)_2]SbF_6$, we integrated the absolute value of the absorption difference $\int |\Delta\alpha| = \int_{\omega_1}^{\omega_2} |\alpha(B) - \alpha(B = 0\ T)| d\omega$ and plotted this data as a function of applied field [Fig. 2 (g)]. Here, $\Delta\alpha$ is the field-induced absorption difference, B is magnetic field, and ω_1 and ω_2 are the frequency limits of integration. These values follow the magnetization squared[31] for both the pyrazine out-of-plane and HF_2^- modes [Fig. 2 (g)]. This trend and the pattern of predicted spin densities [Fig. 2 (c,d)] mirror those found in $[Cu(HF_2)(pyz)_2]BF_4$ and $Cu(pyz)(NO_3)_2$ where the pyrazine ring also distorts proportionally to the magnetization squared.[10,11] What is different about $[Ni(HF_2)(pyz)_2]SbF_6$ is that field-induced absorption differences related to changes in the HF_2^- modes indicate that this ligand must also distort in order to stabilize the fully polarized state. That it does so as the square of

the magnetization points to the generality of this type of mechanism across a quantum phase transition.[31] Moreover, it is the unique balance of inter- to intra-plane exchange interactions (11.3 K through HF_2^- compared to 1 K for the pyrazine ring)[3] that allows the effect to be observed in $[Ni(HF_2)(pyz)_2]SbF_6$. This finding suggests that other hydrogen bond-based ligands, like $H_2F_3^-$, may participate in magnetoelastic coupling when the relative magnetic energy scales are appropriate.

Revealing a series of pressure-induced structural phase transitions

Pressure is different than magnetic field in that it acts directly on bond lengths and bond angles to reduce the overall volume of the system.[32] Shorter bond lengths and smaller volumes under pressure tend to harden the corresponding vibrational modes, and bond angle strain drives changes in crystal symmetry. Chemical bonding variations also impact magnetism,[33] and it is well known that compression can trigger magnetic crossovers - for instance, from high-to-low spin or from the antiferromagnetic to ferromagnetic state.[34,35] High pressure and high field techniques thus provide complementary platforms with which to untangle spin-lattice interactions.[12,36–38] In order to explore these connections, we measured the infrared response of $[Ni(HF_2)(pyz)_2]SbF_6$ under compression, searching for structural phase transitions that might support emergent magnetic properties.

Figure 3 (a,b,e,f) displays close-up views of the pyrazine out-of-plane bending and HF_2^- bending and asymmetric stretching modes of $[Ni(HF_2)(pyz)_2]SbF_6$ under pressure. Only features related to these ligands show anything other than standard compression-induced hardening, so we focus on frequency shifts, splittings, and mode appearances (or disappearances) that define phase boundaries.[37–40] Tracking the vibrational mode frequencies vs. pressure [Fig. 3 (c,d,g)] reveals a series of three different structural phase transitions at 1, 3, and 6 GPa which we discuss below.

The first pressure-induced transition in $[Ni(HF_2)(pyz)_2]SbF_6$ occurs at $P_{C1} = 1$ GPa. It is clearly signalled by the suppression of the HF_2^- bending mode near 1275 cm^{-1}. Strikingly,

this is the only feature that is sensitive to P_{C1} suggesting that it is merely a local lattice distortion with the crystal structure remaining in the $P4/nmm$ space group. One interaction that might dampen this displacement is weak hydrogen bond formation between HF_2^- and the nearby SbF_6 counterion to pin the central hydrogen center in place. This interaction may also explain the rigidity of this mode under compression [Fig. 3 (g)]. Since the geometries of the superexchange ligands are not significantly altered, we anticipate that the magnetic

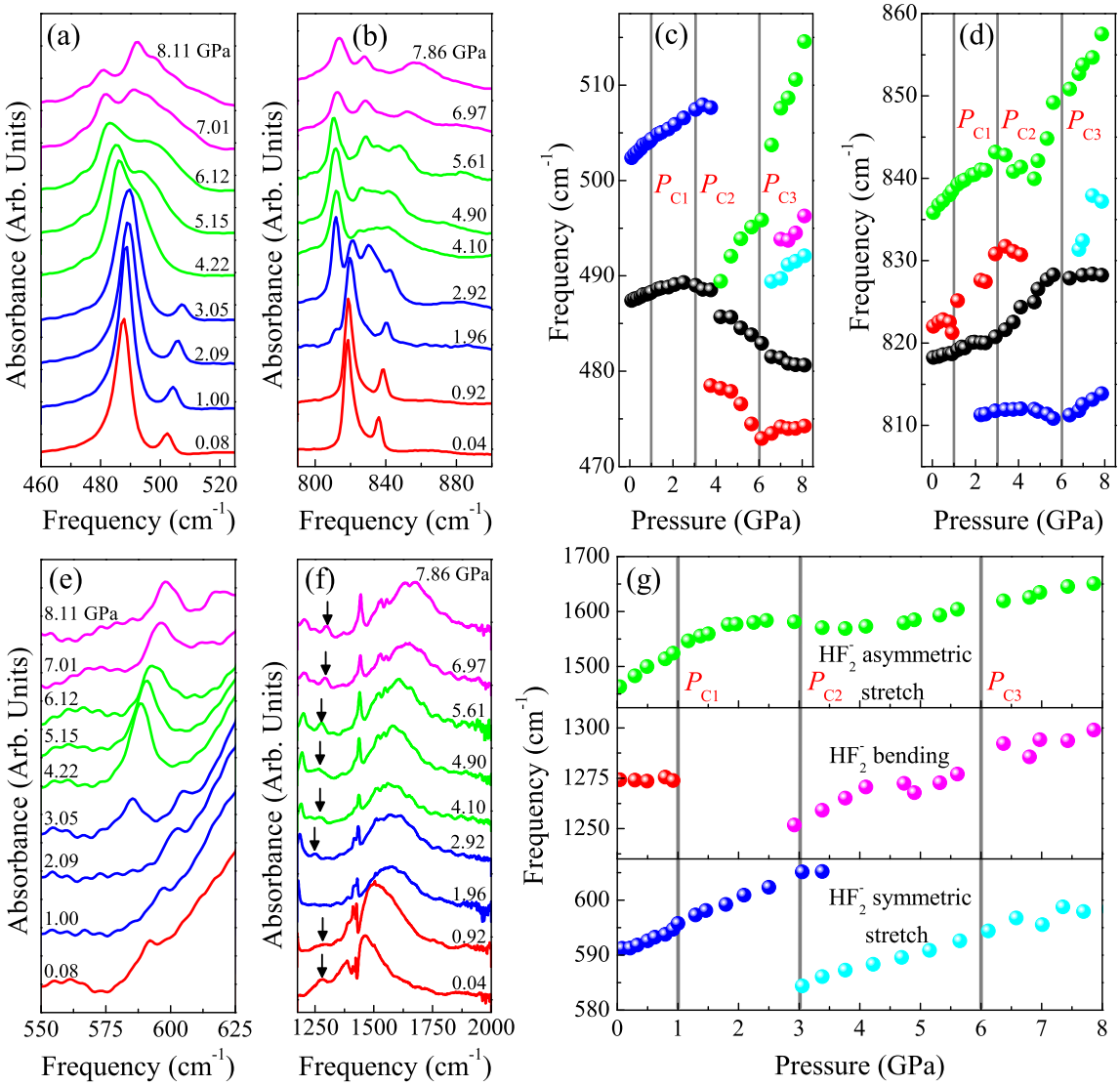

Figure 3: (a,b) Spectra of $[Ni(HF_2)(pyz)_2]SbF_6$ taken at increasing pressure showing the pyrazine out-of-plane modes. (c,d) Frequency versus pressure for the pyrazine features. (e,f) Spectra taken at the indicated pressures in the region of the HF_2^- modes. The arrows indicate the position of the HF_2^- bending mode. (g) Frequency versus pressure for the HF_2^- modes.

properties will not be strongly affected through the 1 GPa transition.

The 3 GPa structural phase transition is the most marked of the series. Both HF_2^- and pyrazine display pronounced distortions making P_{C2} the most likely to drive new properties. For instance, the HF_2^- bending mode that was lost across P_{C1} is recovered at a lower frequency, and the symmetric stretch softens significantly. The asymmetric stretch also reverses behavior and begins to soften under compression (rather than hardening). These pressure vs. frequency trends suggest that the bulk modulus of $[Ni(HF_2)(pyz)_2]SbF_6$ is substantially reduced across the 3 GPa transition. Importantly, the HF_2^- bridge remains symmetric throughout. There is no evidence for modes related to formation of an asymmetric HF_2^- linkage.[27] Based on the frequency shift of the HF_2^- asymmetric stretching mode through P_{C2}, we estimate a 0.08 Å reduction in the H···F bond length. The pyrazine ligands also display pronounced changes through P_{C2}. New modes appear on the low frequency edges of both pyrazine clusters; the 502 cm^{-1} mode disappears, and the out-of-plane mode at 487 cm^{-1} begins to split into a doublet. Taken together, these distortions are consistent with a major reduction in symmetry - probably to a monoclinic space group. Since these ligands form the superexchange pathways in $[Ni(HF_2)(pyz)_2]SbF_6$, we anticipate emergent magnetic properties across P_{C2} - a possibility that merits further investigation. In any case, splitting of the pyrazine out-of-plane bending modes above 3 GPa implies that the ring is strongly distorted - consistent with reduced antiferromagnetic interactions (in analogy to the high field behavior)[10,11] that imply a lower T_N, a reduced critical field, or perhaps even support a crossover to a ferromagnetic state. Other molecule-based materials sport magnetic crossovers in a similar pressure range.[35,36,41]

The pressure-induced phase transition at P_{C3}=6 GPa mainly involves the pyrazine ring. The 480 cm^{-1} out-of-plane C bending mode switches from softening to hardening, two new features appear around 490 cm^{-1}, the 810 cm^{-1} out-of-plane H bending mode of the ring begins to harden, and the 820 cm^{-1} feature splits into a doublet. By contrast, HF_2^--related features display only normal hardening, demonstrating that the HF_2^- linkage is unaffected.

Since additional vibrational structure related to the pyrazine ligands develops through the 6 GPa transition, the rings must be experiencing additional symmetry-breaking distortions. These ring distortions will further reduce the antiferromagnetic exchange between Ni centers, and while they may reduce T_N, they should also lower the critical field - making the quantum phase transition in $[Ni(HF_2)(pyz)_2]SbF_6$ easier to realize.[42]

Structure-property relations

Coordination polymers sport a wide variety of ligands affording opportunities to explore structure-property relations. When pyrazine rings are incorporated into magnetic systems, they are typically the dominant superexchange ligands, even if HF_2^- bridges are present,[1,2] such that little is known about HF_2^- because there have been no opportunities to study it. The situation is different in $[Ni(HF_2)(pyz)_2]SbF_6$[3] making it an ideal system to highlight and investigate the role of the HF_2^- ligand. We find that HF_2^- is a robust, yet sensitive, superexchange ligand in $[Ni(HF_2)(pyz)_2]SbF_6$. This moiety also remains symmetric under different perturbations. To recap, the H···F linkages are known to lengthen at low temperature (from 1.130 Å at 298 K to 1.150 Å at 17 K).[3] Applied magnetic field also lengthens the H···F linkages, although only about one-tenth as much as that under temperature. Compression, of course, shortens the H···F distances. A frequency shift analysis suggests a 0.15 Å reduction of the H···F distance at 9 GPa. These changes are reversible and demonstrate malleability of the HF_2^- ligand despite the strength of the three-center two-electron bonding.

This surprising stability likely arises from the linearity of the Ni-F···H···F-Ni bridge. Non-linear hydrogen bond-based ligands such as $H_2F_3^-$ will deform more easily[2,43] because the angles present an additional route by which to easily alter the magnetic exchange or reduce volume. Although the Goodenough-Kanamori rules dictate that linear bond angles support the strongest antiferromagnetic coupling,[33] incorporating non-linear ligands such as $H_2F_3^-$ may provide additional tunability. Comparison of two structural polymorphs of $[Ni(HF_2)(pyz)_2]PF_6$ demonstrated that HF_2^- supports stronger superexchange when the Ni-

F···H···F-Ni chain is linear.[44] In this case, the lower critical field of the non-linear analog may be due to a combination of weaker exchange and more easily driven lattice distortions. We anticipate the non-linear HF_2^- system to have comparatively lower critical pressures as well since changing the Ni-F···H bond angles would present pathways for readily reducing the unit cell volume. Structural and magnetic stability under external stimuli are therefore increased when the HF_2^- ligand is linear.

Conclusion

In summary, we combined infrared spectroscopy with variable temperature, magnetic field, and pressure techniques to investigate spin-lattice coupling processes in $[Ni(HF_2)(pyz)_2]SbF_6$, a rare system where superexchange in the inter- and intra-layer directions, as represented by the HF_2^- and pyrazine ligands, respectively, are reversed from the typical pattern. Even though it only links the Ni centers in one direction, the HF_2^- ligand surprisingly must relax to reduce antiferromagnetic interactions through the magnetic quantum phase transition, analogous to the known distortions of the pyrazine ring.[10–12] Compression reveals similar processes at work. We find a pressure-induced structural phase transition at 3 GPa that is very likely to modify the magnetic properties as well as more subtle local lattice distortions at 1 and 6 GPa. High pressure magnetization and x-ray measurements are clearly needed to explore the crystal structures and spin arrangements of these new high pressure phases. Taken together, these results indicate that the three-center two-electron bond HF_2^- ligand is surprisingly sensitive to external stimuli, and that its inclusion as a superexchange ligand enhances tunability in transition metal coordination polymers.

Acknowledgments

This work was supported by the National Science Foundation [DMR-1063880 (JLM, UT) and DMR-1306158 (JLM, EWU)] and the Petroleum Research Fund [52052-ND10 (JLM,

UT)]. The National High Magnetic Field Laboratory is supported by the National Science Foundation through NSFDMR-0084173 and the State of Florida. The National Synchrotron Light Source at Brookhaven National Laboratory is funded by the US Department of Energy under Contracts DE-AC98-06CH10886 and DE-FG02-96ER45579. The use of U2A beamline is funded by COMPRES under NSF Cooperative Agreement EAR 11-57758 and CDAC (DE-FC03-03N00144).

References

(1) Goddard, P. A.; Singleton, J.; Sengupta, P.; McDonald, R. D.; Lancaster, T.; Blundell, S. J.; Pratt, F. L.; Cox, S.; Harrison, N.; Manson, J. L.; Southerland, H. I.; Schlueter, J. A. Experimentally determining the exchange parameters of quasi-two-dimensional Heisenberg magets. *New J. Phys.* **2008**, *10*, 083205, DOI: 10.1088/1367-2630/10/8/083025.

(2) Manson, J. L. et al. Strong H···F hydrogen bonds as synthons in polymeric quantum magnets: Structural, magnetic, and theoretical characterization of $[Cu(HF_2)(pyrazine)_2]SbF_6$, $[Cu_2F(HF)(HF_2)(pyrazine)_4](SbF_6)_2$, and $[CuAg(H_3F_4)(pyrazine)_5]$(. *J. Am. Chem. Soc.* **2009**, *131*, 6733–6747, DOI: 10.1021/ja808761d.

(3) Manson, J. L. et al. Structural, electronic, and magnetic properties of quasi-1D quantum magnets $[Ni(HF_2)(pyz)_2]X$ (pyz = pyrazine; X = PF_6^- , SbF_6^-) exhibiting Ni-FHF-Ni and Ni-pyz-Ni spin interactions. *Inorg. Chem.* **2011**, *50*, 5990–6009, DOI: 10.1021/ic102532h.

(4) Here, we employ a single J spin Hamiltonian of the form $\mathcal{H} = -J \sum_{ij} \mathbf{S}_i \cdot \mathbf{S}_j - g\mu_B B \sum_i S_i^z$.

(5) J_{intra} was determined based on expectations in comparing to related quasi–2D Ni–

pyrazine square lattices. J_{inter} was obtained by fitting the magnetic susceptibility data to the Weng chain model as described in Ref. 3.

(6) Brambleby, J. et al. Magnetic ground state of the two isostructual polymeric quantum magnets $[Cu(HF_2)(pyrazine)_2]SbF_6$ and $[Co(HF_2)(pyrazine)_2]SbF_6$ investigated with neutron powder diffraction. *Phys. Rev. B* **2015**, *92*, 134406, DOI: 10.1103/PhysRevB.92.134406.

(7) Liu, J. et al. Antiferromagnetism in a Family of $S = 1$ Square Lattice Coordination Polymers $NiX_2(pyz)_2$ (X = Cl, Br, I, NCS; pyz = Pyrazine). *Inorg. Chem.* **2016**, *55*, 3515–3529, DOI: 10.1021/acs.inorgchem.5b02991.

(8) Manson, J. L.; Conner, M. M.; Schlueter, J. A.; McConnell, A. C.; Southerland, H. I.; Malfant, I.; Lancaster, T.; Blundell, S. J.; Brooks, M. L.; Pratt, F. L.; Singleton, J.; McDonald, R. D.; Lee, C.; Whangbo, M.-H. Experimental and theoretical characterization of the magnetic properties of $CuF_2(H_2O)_2(pyz)$ (pyz = pyrazine): A two-dimensional quantum magnet arising from supersuperexchange interactions through hydrogen bonded paths. *Chem. Mater.* **2008**, *20*, 7408–7416, DOI: Doi␣10.1021/Cm8016566.

(9) Kajňaková, M.; Orendáč, M.; Orendáčová, A.; Vlček, A.; Černák, J.; Kravchyna, O. V.; Anders, A. G.; Bałanda, M.; Park, J. H.; Feher, A.; Meisel, M. W. $Cu(H_2O)_2(C_2H_8N_2)SO_4$: A quasi-two-dimensional $S = \frac{1}{2}$ Heisenberg antiferromagnet. *Phys. Rev. B* **2005**, *71*, 014435, DOI: 10.1103/PhysRevB.71.014435.

(10) Musfeldt, J. L.; Vergara, L. I.; Brinzari, T. V.; Lee, C.; Tung, L. C.; Kang, J.; Wang, Y. J.; Schlueter, J. A.; Manson, J. L.; Whangbo, M. H. Magnetoelastic coupling through the antiferromagnet-to-ferromagnet transition of quasi-two-dimensional $[Cu(HF_2)(pyz)_2]BF_4$ using infrared spectroscopy. *Phys. Rev. Lett.* **2009**, *103*, 157401, DOI: 10.1103/PhysRevLett.103.157401.

(11) Günaydın-Şen, O.; Lee, C.; Tung, L. C.; Chen, P.; Turnbull, M. M.; Landee, C. P.;

Wang, Y. J.; Whangbo, M. H.; Musfeldt, J. L. Spin-lattice interactions through the quantum critical transition in $Cu(pyz)(NO_3)_2$. *Phys. Rev. B* **2010**, *81*, 104307, DOI: 10.1103/PhysRevB.81.104307.

(12) O'Neal, K. R.; Holinsworth, B. S.; Chen, Z.; Peterson, P. K.; Carreiro, K. E.; Lee, C.; Manson, J. L.; Whangbo, M.-H.; Li, Z.; Liu, Z.; Musfeldt, J. L. Spin–lattice coupling in $[Ni(HF_2)(pyrazine)_2]SbF_6$ involving the HF_2^- superexchange pathway. *Inorg. Chem.* **2016**, *55*, 12172–12178, DOI: 10.1021/acs.inorgchem.6b01679.

(13) al-Wahish, A.; O'Neal, K. R.; Lee, C.; Fan, S.; Hughey, K.; Yokosuk, M. O.; Clune, A.; Li, Z.; Manson, J. L.; Whangbo, M.-H.; Musfeldt, J. L., Role of magnetoelastic coupling in magnetic quantum critical transition in Heisenberg antiferromagnetic materials. Submitted to *Phys. Rev. Lett.*

(14) Carr, G. L.; Martin, M. C.; McKinney, W. R.; Jordan, K.; Neil, G. R.; Williams, G. P. High-power terahertz radiation from relativistic electrons. *Nature* **2002**, *420*, 153–156, DOI: 10.1038/nature01175.

(15) Mao, H. K.; Bell, P. M.; Shaner, J. W.; Steinberg, D. J. Specific volume measurements of Cu, Mo, Pd, and Ag and calibration of the ruby R_1 fluorescence pressure gauge from 0.06 to 1 Mbar. *J. Appl. Phys.* **1978**, *49*, 3276–3283, DOI: 10.1063/1.325277.

(16) Blöchl, P. E. Projector augmented-wave method. *Phys. Rev. B* **1994**, *50*, 17953–17979, DOI: 10.1103/PhysRevB.50.17953.

(17) Dudarev, S. L.; Savrasov, S. Y.; Humphreys, C. J.; Sutton, A. P. Electron-energy-loss spectra and the structural stability of nickel oxide: An LSDA+U study. *Phys. Rev. B* **1998**, *57*, 1505–1509, DOI: 10.1103/PhysRevB.57.1505.

(18) Kresse, G.; Joubert, D. From ultrasoft pseudopotentials to the projector augmented-wave method. *Phys. Rev. B* **1999**, *59*, 1758–1775, DOI: 10.1103/PhysRevB.59.1758.

(19) Kresse, G.; Furthmüller, J. Efficient iterative schemes for *ab initio* total-energy calculations using a plane-wave basis set. *Phys. Rev. B* **1996**, *54*, 11169–11186, DOI: 10.1103/PhysRevB.54.11169.

(20) Perdew, J. P.; Burke, K.; Ernzerhof, M. Generalized gradient approximation made simple. *Phys. Rev. Lett.* **1996**, *77*, 3865–3868, DOI: 10.1103/PhysRevLett.77.3865.

(21) See the Supplemental Information for details.

(22) Antoshina, L. G. The behaviour of the magnetostriction and magnetoresistance of the ferrite $CuGa_{0.4}Al_{0.8}Fe_{0.8}O_4$ with frustrated magnetic structure. *J. Phys. Condens. Matter* **2001**, *13*, L127–L133.

(23) Gomonay, H. Magnetoelastic mechanism of long-range magnetic ordering in magnetic/nonmagnetic multilayers. *Phys. Rev. B* **2001**, *64*, 054404, DOI: 10.1103/PhysRevB.64.054404.

(24) Sun, Q. C.; Baker, S. N.; Christianson, A. D.; Musfeldt, J. L. Magnetoelastic coupling in bulk and nanoscale MnO. *Phys. Rev. B* **2011**, *84*, 014301, DOI: 10.1103/PhysRevB.84.014301.

(25) Charilaou, M.; Sheptyakov, D.; Löffler, J. F.; Gehring, A. U. Large spontaneous magnetostriction in $FeTiO_3$ and adjustable magnetic configuration in Fe(III)-doped $FeTiO_3$. *Phys. Rev. B* **2012**, *86*, 024439, DOI: 10.1103/PhysRevB.86.024439.

(26) Casto, L. D.; Clune, A. J.; Yokosuk, M. O.; Musfeldt, J. L.; Williams, T. J.; Zhuang, H. L.; Lin, M. W.; Xiao, K.; Hennig, R. G.; Sales, B. C.; Yan, J. Q.; Mandrus, D. Strong spin-lattice coupling in $CrSiTe_3$. *APL Mater.* **2015**, *3*, 041515, DOI: 10.1063/1.4914134.

(27) Emsley, J. Very strong hydrogen bonding. *Chem. Soc. Rev.* **1980**, *9*, 91–124.

(28) Jones, B. R.; Varughese, P. A.; Olejniczak, I.; Pigos, J. M.; Musfeldt, J. L.; Landee, C. P.; Turnbull, M. M.; Carr, G. L. Vibrational properties of the one-dimensional, $S = 1/2$, Heisenberg antiferromagnet copper pyrazine dinitrate. *Chem. Mater.* **2001**, *13*, 2127–2134.

(29) Freindorf, M.; Kraka, E.; Cremer, D. A comprehensive analysis of hydrogen bond interactions based on local vibrational modes. *Int. J. Quantum Chem.* **2012**, *112*, 3174–3187, DOI: 10.1002/qua.24118.

(30) Manson, J. L.; Schlueter, J. A.; McDonald, R. D.; Singleton, J. Crystal structure and antiferromagnetic ordering of quasi-2D $[Cu(HF_2)(pyz)_2]TaF_6$ (pyz=pyrazine). *J. Low Temp. Phys.* **2010**, *159*, 15–19, DOI: 10.1007/s10909-009-0079-5.

(31) Granado, E.; García, A.; Sanjurjo, J. A.; Rettori, C.; Torriani, I.; Prado, F.; Sánchez, R. D.; Caneiro, A.; Oseroff, S. B. Magnetic ordering effects in the Raman spectra of $La_{1-x}Mn_{1-x}O_3$. *Phys. Rev. B* **1999**, *60*, 11879–11882, DOI: 10.1103/PhysRevB.60.11879.

(32) Grochala, W.; Hoffmann, R.; Feng, J.; Ashcroft, N. W. The chemical imagination at work in very tight places. *Angew. Chemie - Int. Ed.* **2007**, *46*, 3620–3642, DOI: 10.1002/anie.200602485.

(33) Goodenough, J. B. *Magnetism and the chemical bond*; Interscience Publishers: New York-London, 1963; DOI: 10.1017/CBO9781107415324.004.

(34) Shum, W. W.; Her, J. H.; Stephens, P. W.; Lee, Y.; Miller, J. S. Observation of the pressure dependent reversible enhancement of T_c and loss of the anomalous constricted hysteresis for $[Ru_2(O_2CMe)_4]_3[Cr(CN)_6]$. *Adv. Mater.* **2007**, *19*, 2910–2913, DOI: 10.1002/adma.200602751.

(35) Nuttall, C. J.; Takenobu, T.; Iwasa, Y.; Kurmoo, M. Pressure dependence of the mag-

netization of $M^{II}(N(CN)_2)_2$: Mechanism for the Long Range Magnetic Ordering. *Mol. Cryst. Liq. Cryst.* **2000**, *343*, 227–234, DOI: 10.1080/10587250008023531.

(36) O'Neal, K. R.; Liu, Z.; Miller, J. S.; Fishman, R. S.; Musfeldt, J. L. Pressure-driven high-to-low spin transition in the bimetallic quantum magnet $[Ru_2(O_2CMe)_4]_3[Cr(CN)_6]$. *Phys. Rev. B* **2014**, *90*, 104301, DOI: 10.1103/PhysRevB.90.104301.

(37) Brinzari, T. V.; O'Neal, K. R.; Manson, J. L.; Schlueter, J. A.; Litvinchuk, A. P.; Liu, Z.; Musfeldt, J. L. Local lattice distortions in $Mn[N(CN)_2]_2$ under pressure. *Inorg. Chem.* **2016**, *55*, 1956–1961, DOI: 10.1021/acs.inorgchem.5b01870.

(38) Musfeldt, J. L.; Liu, Z.; Li, S.; Kang, J.; Lee, C.; Jena, O.; Manson, J. L.; Schlueter, J. A.; Carr, G. L.; Whangbo, M.-H. Pressure-induced local structure distortions in $Cu(pyz)F_2(H_2O)_2$. *Inorg. Chem.* **2011**, *50*, 6347–6352.

(39) Li, S.; Wang, K.; Zhou, M.; Li, Q.; Liu, B.; Zou, G.; Zou, B. Pressure-induced phase transitions in ammonium squarate: A supramolecular structure based on hydrogen-bonding and π-stacking interactions. *J. Phys. Chem. B* **2011**, *115*, 8981–8988, DOI: 10.1021/jp202975q.

(40) Mączka, M.; Da Silva, T. A.; Paraguassu, W.; Ptak, M.; Hermanowicz, K. Raman and IR studies of pressure- and temperature-induced phase transitions in $[(CH_2)_3NH_2][Zn(HCOO)_3]$. *Inorg. Chem.* **2014**, *53*, 12650–12657, DOI: 10.1021/ic502426x.

(41) Fishman, R. S.; Shum, W. W.; Miller, J. S. Pressure-induced phase transition in a molecule-based magnet with interpenetrating sublattices. *Phys. Rev. B* **2010**, *81*, 172407, DOI: 10.1103/PhysRevB.81.172407.

(42) Ghannadzadeh, S.; Möller, J. S.; Goddard, P. A.; Lancaster, T.; Xiao, F.; Blundell, S. J.; Maisuradze, A.; Khasanov, R.; Manson, J. L.; Tozer, S. W.; Graf, D.;

Schlueter, J. A. Evolution of magnetic interactions in a pressure-induced Jahn-Teller driven magnetic dimensionality switch. *Phys. Rev. B* **2013**, *87*, 241102(R), DOI: 10.1103/PhysRevB.87.241102.

(43) Manson, J. L.; Conner, M. M.; Schlueter, J. A.; Hyzer, K. A. Structural and magnetic properties of quasi-1 and 2D pyrazine-containing spin-1/2 antiferromagnets. *Polyhedron* **2007**, *26*, 1912–1916, DOI: 10.1016/j.poly.2006.09.045.

(44) Manson, J. L. et al. Influence of HF_2 geometry on magnetic interactions elucidated from polymorphs of the metal–organic framework $[Ni(HF_2)(pyz)_2]PF_6$ (pyz = pyrazine). *Dalt. Trans.* **2012**, *41*, 7235–7243, DOI: 10.1039/c2dt30113j.

Graphical TOC Entry